Agricultural Systems 159 (2018) 144–156

Contents lists available at ScienceDirect

Agricultural Systems

journal homepage: www.elsevier.com/locate/agsy

Climate change and dryland wheat systems in the US Pacific Northwest

T. Karimi, C.O. Stöckle*, S. Higgins, R. Nelson

Department of Biological Systems Engineering, Washington State University, Pullman, WA, USA

ARTICLE INFO

Keywords:
Global climate model
Representative concentration pathway
Agroecological zone

ABSTRACT

A regional assessment of baseline (1980–2010) and future (2015–2085) yields of dryland wheat-based cropping systems in the US Inland Pacific Northwest (IPNW) was conducted. The computer simulation-based assessment was done using CropSyst, a cropping systems simulation model, and projected daily weather data downscaled to a 4 × 4 km grid using 12 general circulation models (GCMs) for two atmospheric CO_2 representative concentration pathways (RCP 4.5 and RCP 8.5). The study region was divided into 3 agro-ecological zones (AEZs): continuous cropping (CC), continuous cropping-fallow transition (CCF), and crop-fallow (CF), with the following typical rotations assigned to the zones: winter wheat (WW) – summer fallow (SF) (CF zone), WW – spring wheat (SW) – SF (CCF zone), and WW – SW – spring pea (CC zone). By the 2070s (2065–2085), precipitation in the IPNW is projected to increase by about 8 and 12% compared to the baseline period under RCP 4.5 and 8.5, respectively. Mean temperature during the WW growing season will increase about 1.5 and 2.3 °C under RCP 4.5 and 8.5, respectively, but will not change noticeably during the SW growing season due to the adaptive early planting used in this study. Concurrently, atmospheric CO_2 concentration will increase from today's average of ~400 ppm to 532 ppm to 801 ppm by 2085 depending on future emissions of greenhouse gases. Soil water-crop growth interactions, which show large variation across the region, will modulate crop responses to these changing conditions, with our results showing an overall increase in yield across the IPNW. By the 2070s, the mean ratio of future to baseline WW yield will range from 1.29 to 1.35 under RCP 4.5 and from 1.41 to 1.64 under RCP 8.5 depending on the AEZ. The mean yield ratio for SW across AEZs will range from 1.38 to 1.53 under RCP 4.5 and 1.54 to 1.91 under RCP 8.5. Given substantial climatic heterogeneity in the region, these gains will not be distributed equally across the region or within AEZs, and overall they will not be shared equally by all growers.

1. Introduction

Climate change presents challenges new to the world's growing human population (Ericksen et al., 2009). With the population projected to reach 11 billion by 2100 (United Nations, 2015), an accurate estimation of major crop yields such as wheat is needed to assess food security (Shewry and Hey, 2015). A global reduction of wheat production is projected as a result of warming and changes in precipitation (Asseng et al., 2011, 2015), but the outlook is more varied and complex when both climate change and rising atmospheric CO_2 concentration are considered, with positive and negative outcomes expressed globally (Ortiz et al., 2008; Wilcox and Makowski, 2014).

Crop vulnerability to climate change and the capacity of agriculture to adapt to new conditions vary regionally. Some regions will experience yield improvements while others will experience declines (Kristensen et al., 2011; Laurila, 2008; Olesen et al., 2011). In a meta-analysis of simulation studies evaluating the effects of climate change on wheat yields (Wilcox and Makowski, 2014), yield decreased in more than 50% of studies if the mean temperature change was higher than 2.3 °C, or if precipitation did not increase in the future. High atmospheric CO_2 could compensate for the effects of temperature and moderate declines in precipitation.

Agriculture contributes to a major portion of the economy in the climatically diverse Inland Pacific Northwest (IPNW) region of the US. Around 17% of the nation's wheat is produced in Oregon, Washington, and Idaho (USDA). Although some parts of the IPNW have very low precipitation, cereal based dryland cropping systems have long existed in this region (Schillinger and Papendick, 2008).

The IPNW has historically experienced relatively wet winters and dry summers. A wide range of precipitation and temperature regimes exist across the IPNW, with annual precipitation ranging from 180 mm to 1130 mm, and temperatures fluctuating largely in response to elevation and local topography. Climate change is expected to bring warmer and dryer summers in the IPNW, and temperature and

* Corresponding author.
E-mail address: stockle@wsu.edu (C.O. Stöckle).

http://dx.doi.org/10.1016/j.agsy.2017.03.014
Received 6 January 2017; Received in revised form 25 February 2017; Accepted 13 March 2017
Available online 06 April 2017

precipitation increases during other seasons. In the IPNW, CMIP5 (fifth phase of the Coupled Model Inter-Comparison Project) models project a mean annual warming of 1.1 °C to 4.7 °C by 2041–2070 compared to the base period of 1950–1999 (Dalton et al., 2013). The frost-free season and the number of hot days are expected to increase with larger increases in the west and southeastern regions. The overall annual change in precipitation is projected to range from − 4.7% to + 13.5% (Creighton et al., 2015; Dalton et al., 2013).

Despite this variation in current and future climatic conditions across the region and potential deleterious effects for agriculture, rising atmospheric CO_2 concentration might counterbalance climate change effects and result in a more positive outcome. Elevated atmospheric CO_2 increases photosynthetic rate (CO_2 fertilization effect) in C_3 plants like wheat (Drake et al., 1997), and reduces stomatal conductance and plant transpiration thus enhancing crop water use efficiency which boosts dryland yields (Ainsworth and Long, 2005).

Few studies have looked at the yields in IPNW under climate change. Thomson et al. (2002) simulated baseline and future WW production in eastern Washington, northeastern Oregon and northwestern Idaho, using just one general circulation model (GCM), two constant CO_2 concentrations for baseline (365 ppm) and future (560 ppm) scenarios, and sixteen grid cells (90 km × km) across the region. Wheat yields for the baseline averaged 4.52 mg ha^{-1} across the study region (including irrigated farms), increasing to 5.45 mg ha^{-1} for the future CO_2 condition. In another study (Stöckle et al., 2010), four representative locations in Washington State were evaluated using four GCMs. Winter wheat yield was projected to increase 13–15% by 2020 and 23–35% by 2080, with larger gains predicted on drier sites. Spring wheat yields only increased about 7% by 2020 and 2% by 2040 in high rainfall areas and declined by 7% by 2040 in the lower rainfall zone without any adaptation strategies. When spring wheat was planted 2 weeks earlier, by 2040 yield increased 11% in the high rainfall zone and 3% in the lower rainfall zone (Stöckle et al., 2010).

Although existing projections provide helpful information about the effect of climate change on IPNW dryland agriculture, the existence of a large precipitation gradient and fluctuating temperature conditions throughout the region, dictating zones with varying degree of crop intensity and use of fallow, generates a heterogeneous system that has not been accounted for by previous work. In addition, the large variation in weather projections of available GCMs implies that the use of a few GCMs in these studies does not reflect the underlying uncertainty that exists. Our objective is to provide a more detailed regional analysis at a high resolution and incorporating a larger number of weather projections, which will lead to a richer understanding of the variable impact of climate change in the IPNW.

2. Materials and methods

Wheat-based dryland cropping systems in the IPNW are closely associated with annual precipitation. The region is customarily classified into three agro-ecological zones (AEZ) (Douglas et al., 1992; Huggins et al., 2011): continuous cropping (CC), continuous cropping to fallow transition (CCF), and crop-fallow (CF). The CC zone is roughly comprised of the area with an annual precipitation of 450 to 1000 mm where annual cropping is feasible. In the CCF zone, with precipitation ranging from about 304 to 457 mm, a fallow period before winter wheat (WW) is necessary to ensure good yields, with WW typically followed by spring wheat (SW), a shorter season crop with lower water demand. The precipitation range in the CF zone is from 180 to 304 mm, which is too low to support annual cropping, and WW is typically planted every other year. The regional distribution of these AEZs is presented in Fig. 1, showing a distinctive east-west pattern. The upper-right corner of the figure situates the study region comprising mainly Washington State, but also including portions of Oregon and Idaho. Typical crop rotations in each AEZ were considered in this study (Table 1). More information on cropping systems in the IPNW can be found in Schillinger et al. (2003).

A 4 × 4 km grid was used to represent the regional climate variation, and downscaled gridded daily weather data from 12 GCMs (Abatzoglou and Brown, 2012) for the period 2015–2085 were used to drive the cropping system simulations. In this study we considered two RCPs including 4.5 and 8.5 Wm^{-2}. As baseline, gridded weather data for the period 1980–2010 were used, which were generated by combining attributes of two datasets: temporally rich data from the North American Land Data Assimilation System Phase 2 and spatially rich data from the Parameter-elevation Regressions on Independent Slopes Model (PRISM) (Abatzoglou, 2013). The previously prepared weather data set includes daily maximum/minimum temperature, precipitation, solar radiation, maximum/minimum humidity, and wind speed.

The USDA-NRCS STATSGO soil data base was used to obtain representative soil data required by CropSyst for each grid cell. Within each 4 × 4 km grid cell, the predominant cropland soil was chosen as an input to the model. Cropland data layers from 2007 to 2011 at a 30 × 30 m resolution (USDA - National Agricultural Statistics Service) were used to determine the fraction of cropland in each 4 × 4 cell. The sand fraction of the soils decreases from west to east while the fine fraction increases from west to east.

Crop simulations were performed using CropSyst (Stöckle et al., 1994; Stöckle et al., 2003), a cropping system model that has been widely used for climate change assessment studies under different climatic conditions around the world (e.g., Bocchiola et al., 2013; Donatelli et al., 2015; Jalota and Vashisht, 2016; Sommer et al., 2013; Torriani et al., 2007). Biomass production as a function of elevated CO_2 is approximated using a non-rectangular hyperbola function (e.g., Thornley, 1998), stomatal conductance is reduced by increasing CO_2 as presented in Allen (1990), and actual transpiration responds to soil water potential and water vapor atmospheric demand as described in Stöckle and Jara (1998). Other details are given by Stöckle et al. (2003). The ability of CropSyst to simulate wheat under elevated CO_2 has been recently confirmed using data from the Australian Grains Free-Air CO_2 Enrichment experiment (located in a semi-arid environment) (O'Leary et al., 2014).

For the current study, all rotations were managed as reduced tillage. A sweep plow was simulated prior to seeding for all crops. After WW harvest in CC and CCF, the soil was chisel plowed. The CropSyst model was used in automatic N fertilization mode, which had the effect of eliminating N stress. Pest and disease pressure were not modeled. Because many wheat varieties are grown in the region, for this system analysis study a “representative” cultivar was defined that conformed to the typical growing season and canopy ground cover in each AEZ. Generalized phenology and yield information (Papendick, 1996; Schillinger et al., 2006; personal communication) was used to adjust crop phenology parameters to simulate the phenology characteristic of the respective zone. For the most part, default parameters for wheat were used throughout the region. Minor adjustment of two WW parameters was done, one to reflect lower canopy coverage at the lower precipitation zone, and the other to reflect a slightly higher yield potential in the higher rainfall zone.

Simulations during a 30-year period (1980–2010) using historic weather records for 5 sites in the region that represented low, medium, and high precipitation zones were performed. The good agreement of simulated and observed yields from independent research conducted in the region indicated that the model could capture the yield differences among sites with very different annual precipitation amounts as well as yield differences between WW and SW cultivars (Table 2).

Within an AEZ, WW was sown on the same day regardless of scenario; day of year 243 in CF, 257 in CCF and 280 in CC. Seeding spring crops, however, depended on 15-day average temperature exceeding a required threshold beginning on March 1. This conditional mode of seeding was adopted only for the spring crops because early spring temperatures are expected to shift substantially as the century

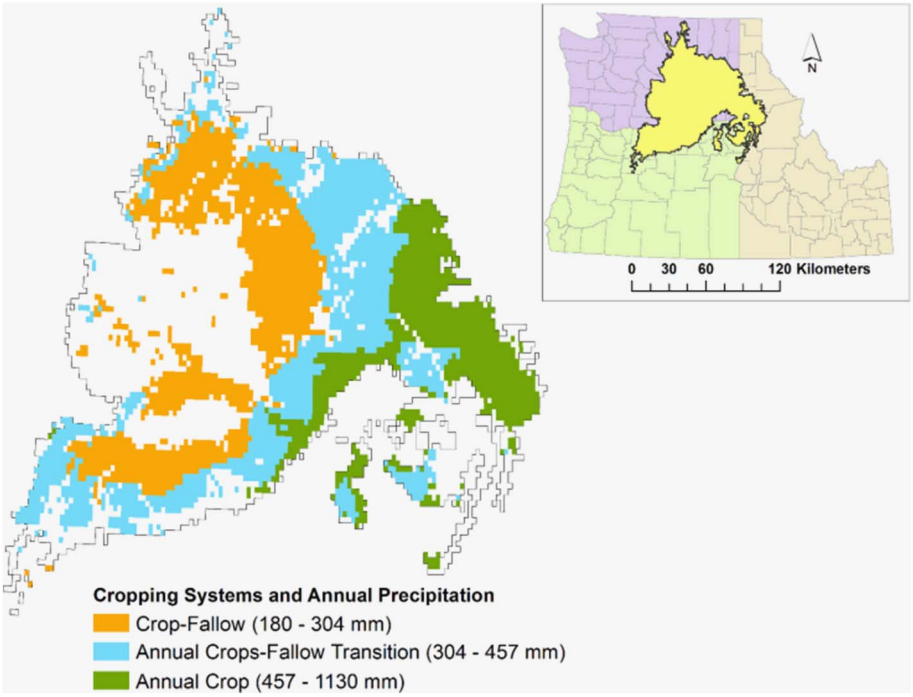

Fig. 1. Inland Pacific Northwest study area showing 3 agroecological zones which are based on annual precipitation ranges. (Single column-colored).

Table 1
Typical rotations simulated in 3 agroecological zones (AEZ) in the Inland Pacific Northwest.

AEZ	Rotation
Continuous cropping	Winter wheat – spring wheat – spring pea
Annual crop-fallow transition	Winter wheat – spring wheat – summer fallow
Crop fallow	Winter wheat – summer fallow

Table 2
Simulated historic wheat yields for several sites in the Inland Pacific Northwest along with measured yields taken from http://smallgrains.wsu.edu/variety/2015-data/ (accessed 1-27-17). Measured yields are from within the same rainfall zone as the tabled location, but not necessarily from the same location.

Location	Annual precipitation (mm)	Winter wheat		Spring wheat	
		Simulated historic yields (Mg ha^{-1})	Measured yields (Mg ha^{-1})	Simulated historic yields (Mg ha^{-1})	Measured yields (Mg ha^{-1})
Moscow Mt.	748	6.56	6.40	4.37	4.07
Pullman	572	6.30	6.40	4.11	4.07
St. John	442	6.10	6.16	3.58	3.59
Wilke	345	5.06	5.40	2.84	2.73
Lind	253	3.09	2.96		

progresses which would allow earlier planting.

Ordinarily in a 3-year crop rotation, each crop would grow in only one third of the years. In our simulations, however, each crop grew in each year of the simulation. A 3-year rotation, e.g., WW-SW-SP (Table 1), was run 3 times, each time starting with a different lead crop in the rotation. In the crop fallow AEZ, the scenario was run twice, once with WW planted in the first year and once with SF in the first year. In this manner, all crops were subjected to every year available in a given location's weather file. For the baseline (1980–2010) and future (2015–2085) periods, once a simulation run was initiated, it ran continuously from one year to the next without reinitializing each year. For the analysis, three overlapping future time periods were established, 2015 to 2045, 2035 to 2065 and 2055 to 2085 which, for convenience, are nominally referred to as 2030, 2050 and 2070. Means of response variables within these time periods were averaged over the respective time period and GCMs within RCP or AEZ as appropriate. Histograms of the frequency distributions of yield for the 4 × 4 km grid cells within crop, RCP and time period were constructed using uniform bin widths (within a crop). The bar height represents the percentage of grid cells in the respective AEZ whose yield fell within that bin.

3. Results and discussion

Environmental conditions and simulated crop responses will be presented separately for winter and spring wheat, and for baseline and future projections, and crop responses to climate change will be discussed. The focus here is on wheat, and responses of spring peas, a rotational crop in the CC zone, will not be presented.

3.1. Winter wheat: Baseline period

3.1.1. Environmental conditions

The average temperature during the WW growing seasons across all the grid cells within each zone over the 31-year (1980–2010) baseline period were 7.3, 7.6 and 8.2 °C in the CC, CCF and CF zones, respectively. The zonal average maximum and minimum temperatures were about 13 and 1.6 °C for CC, 13.5 and 1.7 °C for CCF and 14.3 and 2.3 °C for CF. Fig. 2-a, b, c shows the spatial distribution of baseline average temperature for CC, CCF and CF. Baseline temperatures tended to be cooler in the more northern latitudes of the study area, and warmer moving westward within the study area. The influence of the Columbia River was apparent in the southern portion of the CCF AEZ which extends westward of, and was cooler than the southern portion of the CF AEZ.

The annual baseline precipitation across the study area ranged from 180 to 1130 mm (Fig. 3-a). This large gradient over such a short distance is due to the combination of the rain shadow effect of the Cascade Mountains in the western region of the IPNW and the orographic effect as weather systems move eastward and upward toward the Rocky Mountains east of the IPNW. The zonal average

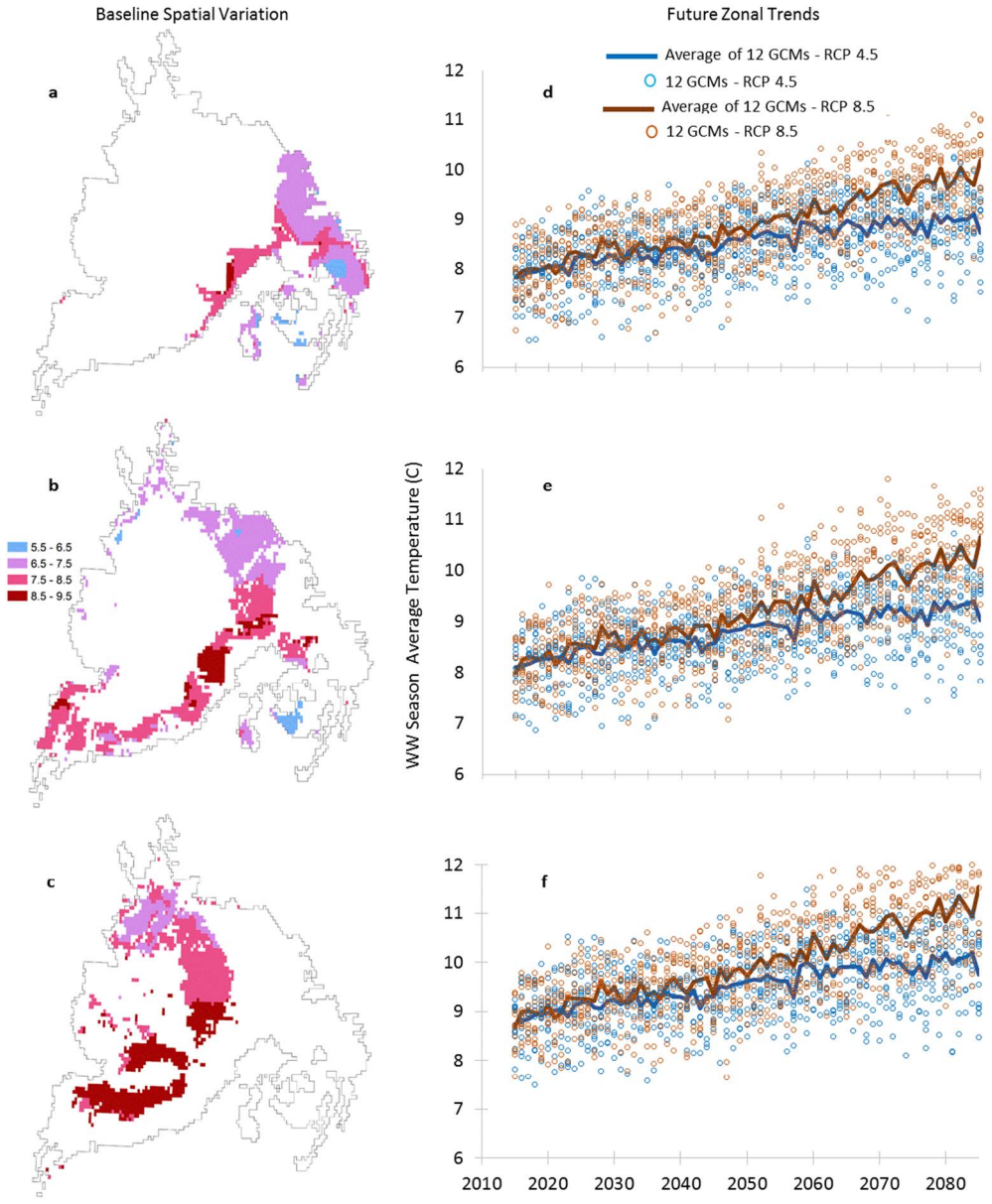

Fig. 2. Spatial distribution of baseline (1980–2010) average temperature during the winter wheat (WW) growing season for the continuous cropping (a), annual crop-fallow transition (b) and crop-fallow (c) agroecological zones (AEZ), and future WW season temperature trends for the same AEZs (d, e and f), averaged over 12 general climate models (GCMs), for 2 atmospheric CO_2 representative concentration pathways (RCP) for the Inland Pacific Northwest. (1.5 column-colored).

annual precipitation and their standard deviation (SD) were 573 ± 90, 373 ± 74 and 257 ± 62 mm for CC, CCF and CF, respectively, with 524, 349 and 244 mm occurring during WW growing seasons (about 91, 94 and 95%) respectively.

3.1.2. Crop response to baseline environmental conditions

Season length was variable across the region given differences in temperature among and within zones (Fig. 2 a,b,c). The zonal average WW season lengths from planting to maturity and their SDs were 295 ± 7, 291 ± 6 and 306 ± 6 days in the CC, CCF and CF zones. The season length in CF was longer than the other zones since the planting date was earlier.

Fig. 4-a, b, c and Fig. 5-a, b, c, show the distribution of baseline actual crop evapotranspiration (ET_a) and transpiration-use efficiency (TUE, expressed as g above-ground biomass produced per kg of water transpired) in each AEZ. Regional variations, primarily of precipitation and also temperature, have a significant effect on ET_a. The zonal average ET_a were 498 ± 61, 377 ± 50 and 281 ± 57 mm at CC, CCF and CF zones, respectively, decreasing from the eastern edge of the study area moving westward. It may seem counterintuitive that WW season ET_a in the CCF and CF zones could exceed annual precipitation, but in both zones WW follows summer fallow so has the advantage of stored soil moisture. There was a wide ET_a range across the study area, from 160 to 550 mm, which will have an important influence on crop response to climate change and elevated CO_2 across the region. The zonal average water stress (a value of zero for no stress and 1 for maximum possible stress) experienced by WW during the growing season was similar in CC and CCF (0.13 and 0.14) and higher in CF (0.22) which had the lowest precipitation, indicating that all zones were affected by water deficit. The zonal average seasonal TUE for WW was similar in all 3 zones, 4.8 ± 0.26, 5.0 ± 0.27and 4.9 ± 0.3 g biomass kg water^{-1} in the CC, CCF and CF zones, respectively, but with spatial variations within zones. In each zone, there tended to be a preponderance of lower TUE in the northern portion of the zone (Fig. 5-a, b, c). Factors such as higher early season temperature and greater severity of water stress toward the end of the season in southern

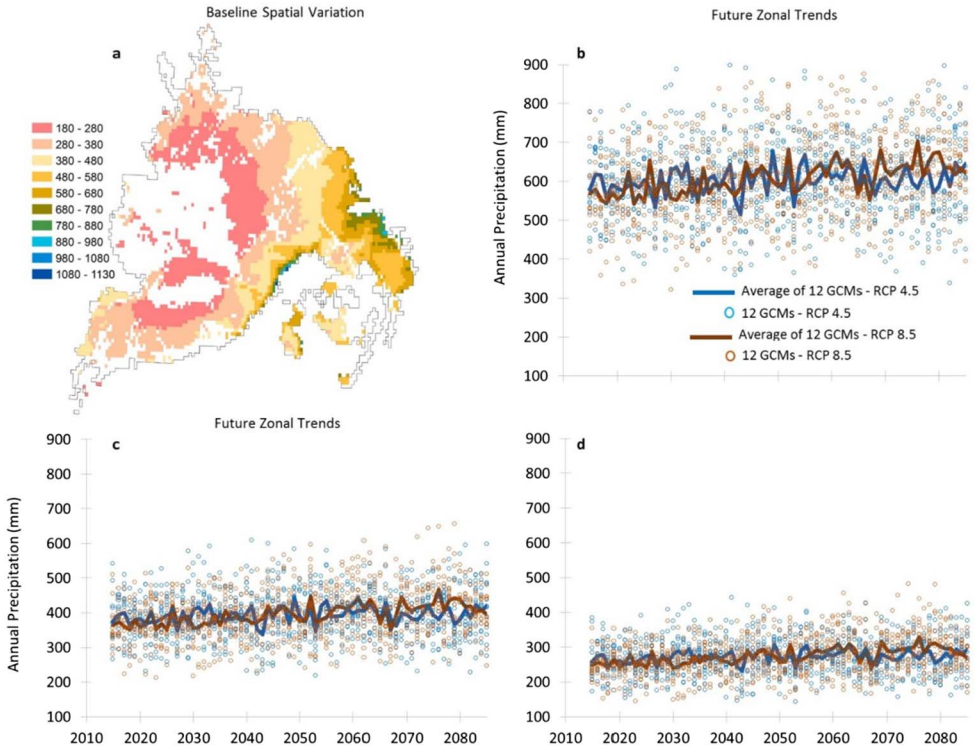

Fig. 3. Spatial distribution of baseline (1980–2010) average annual precipitation (mm) for the the Inland Pacific Northwest (a), and future annual precipitation projected for the continuous cropping (b), annual crop-fallow transition (c) and crop-fallow (d) agroecological zones, averaged over 12 general climate models (GCMs), for 2 atmospheric CO_2 representative concentration pathways (RCP). (1.5 column-colored).

portions define these responses, the latter shortening the "effective growing season" so that most growth takes place earlier in the season when lower temperature and vapor pressure deficit favors greater TUE (Kremer et al., 2008). TUE for wheat in Australia based on grain biomass was 1.72 g grain kg water^{-1} (O'Leary et al., 2011). For comparison, we converted our TUE to g grain kg water^{-1} by multiplying by the harvest index, and got 1.98, 1.95 and 1.81 g grain kg water^{-1} for the CC, CCF and CF AEZs, respectively, all somewhat higher than recorded in Australia.

The baseline zonal average of WW yield and their SDs in CC, CCF and CF zones were 5515 ± 1200, 4460 ± 966 and 2765 ± 913 kg ha^{-1}, respectively. Yields were positively correlated to transpiration and available profile soil water at planting, and negatively correlated to crop water stress during the season in CC and CCF. The yields in CF had the same relations but the correlation with available water at planting was lower. The open bars of Fig. 9 show the spatial distribution of baseline WW yield for the different cropping systems. The modal yield is higher in CF, and the distribution, are tighter than in the other AEZs, which could be due to the more stressful CF environment providing fewer options for plant responses.

3.2. Winter wheat: Future periods

3.2.1. Environmental conditions

Fig. 2-d, e, f shows the projected trend of WW season temperature for the period 2015–2085 averaged across all pixels in each zone and the 12 GCM projections. There is a large variation associated with GCMs represented by circles for each year, but the trends are distinctive for RCP4.5 and 8.5. The zonal average WW season temperature will increase about 1.5 °C by the 2070s in all zones under RCP 4.5, and about 2.3 °C under RCP 8.5. Average of minimum season temperature at 2070s will increase about 2 °C in CC and CCF, and about 1.2 °C in CF zone compared to baseline under RCP 4.5, and about 2.7 °C under RCP 8.5 across the entire region (data not shown). The maximum season temperature will increase about 1 °C in all zones under RCP 4.5 and about 1.6, 1.8 and 2.1 °C in CC, CCF and CF zones under RCP 8.5, respectively (data not shown). The range of WW season temperatures predicted by the 12 GCMs within a zone and RCP will tend to increase somewhat between 2015 and 2085 (Fig. 2).

Fig. 3-b, c, d shows the projected trend of zonal annual mean precipitation for the period 2015–2085 based on the 12 GCMs. By the end of the 2070s the zonal average annual precipitation will increase about 7% and 11% under RCP 4.5 and 8.5 in CC and CCF, which is slightly less than the increase in CF (8 and 13%, respectively). Increases in annual precipitation will increase the soil available water for WW growth which is important in dryland agriculture. The projected increase in precipitation is consistent with Dalton et al. (2013) who predicted increased precipitation throughout the IPNW. Under RCP 4.5 and by 2070s, about 90, 91 and 92% of the zonal annual precipitation would occur during the WW growing season in CC, CCF and CF, respectively. These proportions would be less under RCP 8.5 which are about 88% in CC and CCF and 90% in CF. Among the 12 GCMs, the range within a zone generally does not change a great deal between 2015 and 2085 (Fig. 3).

3.2.2. Crop response to future environmental conditions

Higher temperatures shorten the growing season, reducing the amount of intercepted light and thus photosynthesis and biomass production (Asseng et al., 2015). Supra optimal temperatures also increase the risk of heat stress at critical crop growth stages, e.g., flowering (Lipiec et al., 2013; Semenov and Shewry, 2011), and could negatively impact crop production (Zheng et al., 2012; Teixeira et al., 2013). The zonal average WW season length will be reduced by 27, 26 and 11 days under RCP 4.5 by the end of 2070s in CC, CCF and CF zones due to warming, and will be approximately an additional 11 days shorter under RCP 8.5. Because there will be a greater increase in minimum temperature than maximum temperature during the growing season, the accumulation of thermal time during winter will be more rapid for winter wheat. Higher temperature can be beneficial for winter wheat if it advances early growth and reduces the risk of extreme frost

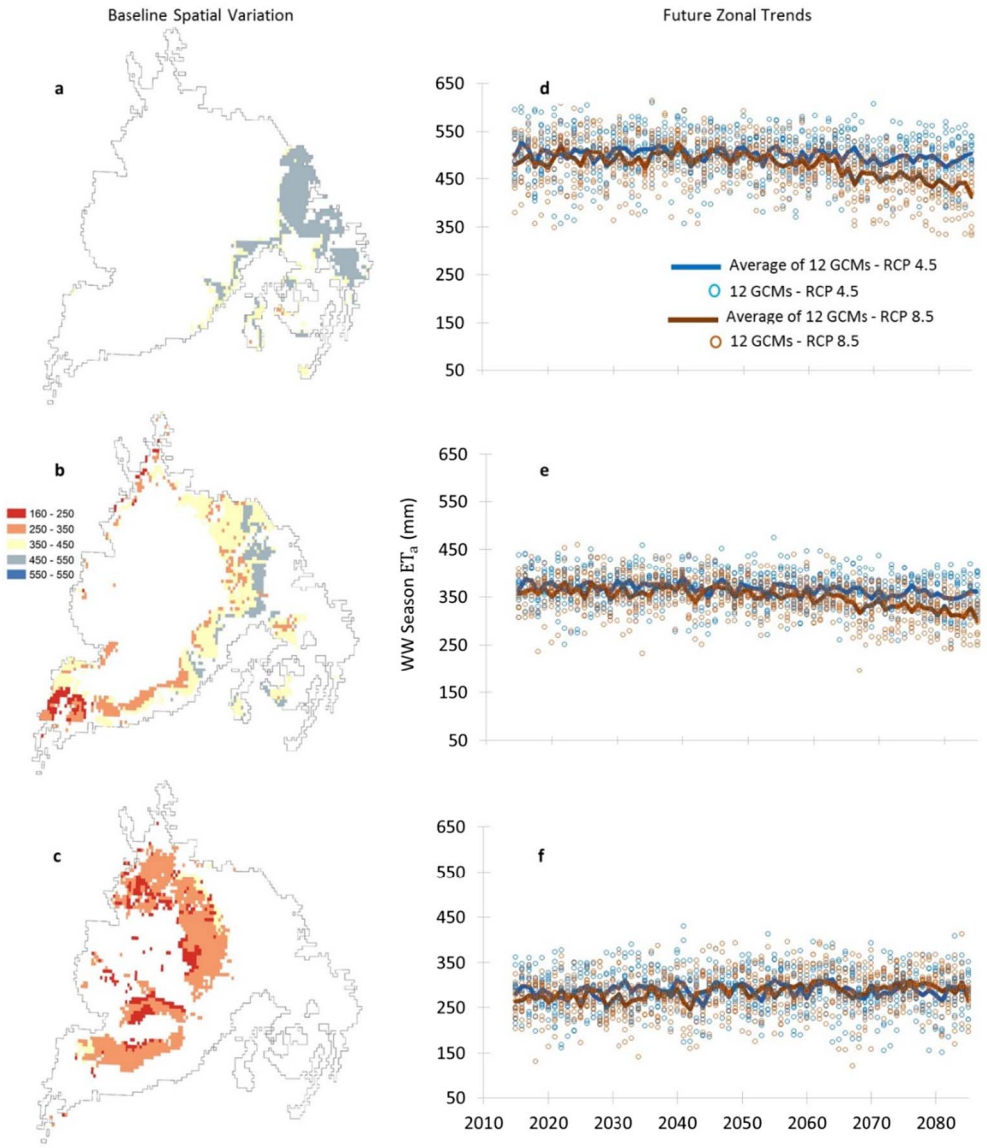

Fig. 4. Spatial distribution of simulated baseline (1980–2010) evapotranspiration (ET_a) during the winter wheat (WW) growing season for the continuous cropping (a), annual crop-fallow transition (b) and crop-fallow (c) agroecological zones (AEZ), and future WW season ET_a trends for the same AEZs (d, e and f), averaged over 12 general climate models (GCMs), for 2 atmospheric CO_2 representative concentration pathways (RCP) for the Inland Pacific Northwest. (1.5 column-colored).

events (Sommer et al., 2013). The compressed growing season will move anthesis earlier in the year, which will reduce the probability that extreme temperatures will endanger seed set.

The trend of WW zonal average ET_a essentially had a slope of zero until mid-century when it started decreasing (Fig. 4). This was the case in both CC and CCF, with ET_a decreasing by 2.7% and 5.3% for RCP 4.5, respectively, and 10.6% and 12.7% for RCP 8.5. In CF, ET_a remained unchanged in RCP 4.5 and increased 8% in RCP 8.5. A small increase in regional precipitation and a rise in temperature that boosted atmospheric evaporative demand contributed to increased potential ET. But this increase was counteracted by elevated atmospheric CO_2 that reduced stomatal conductance (Long et al., 2004; Ainsworth and Long, 2005) and by shortening of the growing season (Asseng et al., 2015). Open field experiments using Free-Air CO_2 Enrichment (FACE) systems (only accounting for CO_2 effects) at Maricopa, Arizona have shown 6.7% lower spring wheat ET_a in plots with elevated CO_2 (550 ppm) compared to ambient (~360 ppm) (Kimball et al., 1999). Also at Maricopa, FACE experiments with sorghum (a C_4 crop) resulted in 10% reduction of ET_a when [CO_2] was elevated from 370 to 570 ppm (Conley et al., 2001).

The combination of the CO_2 effect and shorter growing season explains the midcentury ET_a decline in CC and CCF. In CF, a low precipitation zone, ET_a is limited by water rather than the length of the growing season so that increasing precipitation throughout the century resulted in sustained (RCP 4.5) or increased (RCP 8.5) ET_a. As a result of declining ET_a and greater precipitation, the average soil profile water depth at harvest by the end of the 2070s was 665 mm (RCP 4.5) and 713 mm (RCP 8.5) for the CC zone compared to 580 mm for the baseline, and 388 mm (RCP 4.5) and 420 mm (RCP 8.5) versus 317 mm for the baseline in the CCF zone. This is substantial conservation of water which may provide opportunity for crop intensification in the highest precipitation portions of the study region. In contrast, in the CF zone, the average soil profile water depth at harvest was 308 (RCP 4.5) and 313 mm (RCP 8.5) by the end of the 2070s, essentially the same value of the baseline period (305 mm).

Zonal average TUE had an increasing trend in all zones and reached 6, 6.3 and 6.1 g biomass kg water^{-1} by the 2070s in CC, CCF and CF, respectively, under RCP 4.5 (Fig. 5-d, e, f). The increase was higher under RCP 8.5 by over 1 g biomass kg water^{-1} as a result of a greater CO_2 fertilization effect. Yang et al. (2015) reported an increase of 0.11

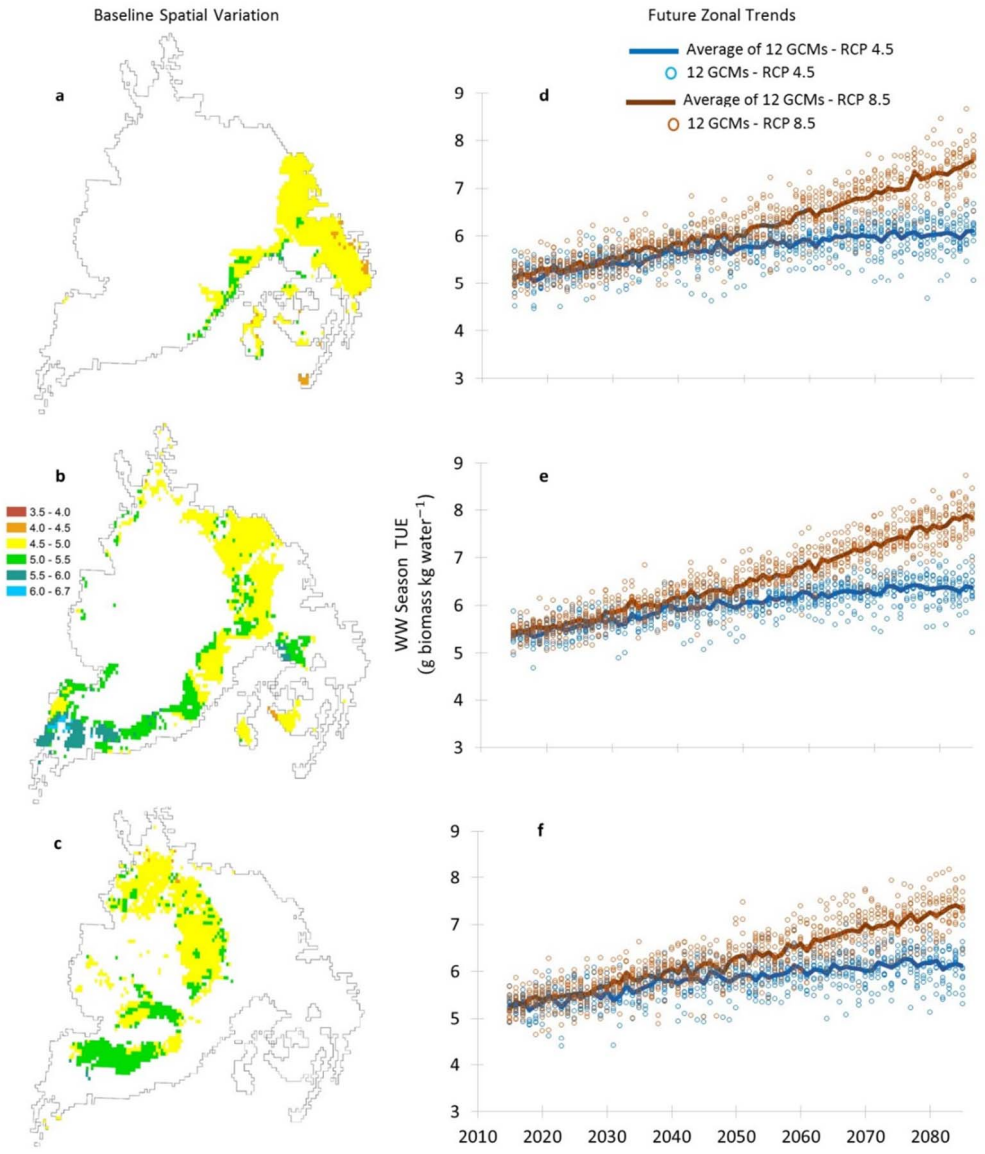

Fig. 5. Spatial distribution of simulated baseline (1980–2010) transpiration use efficiency (TUE) during the winter wheat (WW) growing season for the continuous cropping (a), annual crop-fallow transition (b) and crop-fallow (c) agroecological zones (AEZ), and future WW season TUE trends for the same AEZs (d, e and f), averaged over 12 general climate models (GCMs), for 2 atmospheric CO_2 representative concentration pathways (RCP) for the Inland Pacific Northwest. (1.5 column-colored).

to 0.16 g yield kg water^{-1} TUE in semi-arid southeastern Australia by 2040. Our 2040 data converted to g yield kg water^{-1} were about 0.24 g yield kg water^{-1} for CC and CCF and about 0.17 g yield kg-water^{-1} for CF for RCP 4.5.

Shifts in water balance components, as those discussed above, which influence crop water demand and supply under rainfed conditions are important factors that can impact crop growth and yield (O'Leary et al., 2011; Yang et al., 2015). Table 3 presents the zonal WW yields for RCP 4.5 and 8.5 scenarios, averaged across all GCMs and distributed among 3 time periods (2015–2045, 2035–2065, 2065–2085). In addition, the ratios of future to baseline yields (R) are also presented. The columns labeled Min and Max show the smaller and larger value from all GCMs for each category. The R values which are higher than and less than 1 reveal gains and declines in future WW yields, respectively, over baseline yields. As a result of CO_2 fertilization, WW yields in all zones will continuously increase in each future period considered compared to the baseline, and this effect will be higher under RCP 8.5. The increases in R were slightly higher under RCP 8.5 in CF zone. Since CF is the driest zone, where growth is limited by water rather than season length, the increase in TUE will provide a more effective compensation for the limited water supply (e.g., Grant et al., 1999; Manderscheid and Weigel, 2007). The range provided by the minimum and maximum column values in Table 3 are indicative of the substantial uncertainty associated with GCM projections, but the average trends are clear.

3.3. Spring wheat: Baseline period

3.3.1. Environmental conditions

Fig. 6-a, b, shows the distribution of baseline average temperature during the SW growing season for CC and CCF. Unlike the baseline WW temperatures which tended to be higher at lower latitudes (Fig. 2), SW baseline temperatures tended to be higher at the higher latitudes in the region (Fig. 6-a,b). The zonal average of maximum, minimum and mean temperatures during the SW season were about 22, 7 and 14 °C, respectively, in both the CC and CCF zones. The spatial mean SW seasonal temperature ranged from 13.5 to 15.25 °C across the study region.

The annual baseline precipitation across the study area was already presented (Fig. 3-a). About 30% of the zonal average of annual

Table 3
Zonal winter wheat yield and future to baseline yield ratio averaged across 12 global climate models (GCMs), and minimum and maximum of all GCMs for a given response variable for 2 representative concentration pathways (RCP) in the inland Pacific Northwest. Each period is 31 years, centered on the nominal value, and the zones are the continuous cropping (CC), annual crop-fallow transition (CCF) and crop-fallow (CF) agroecological zones.

Zone	RCP	Period	Yield (kg ha^{-1})			Ratio of future to baseline yield		
			Min	Max	Average	Min	Max	Average
CC	4.5	2030	6300	6867	6608	1.14	1.25	1.20
		2050	6881	7529	7195	1.25	1.37	1.30
		2070	7075	8192	7462	1.28	1.49	1.35
	8.5	2030	6062	6916	6499	1.10	1.25	1.18
		2050	7037	8073	7504	1.28	1.46	1.36
		2070	7096	8959	8063	1.29	1.62	1.46
CCF	4.5	2030	4898	5443	5153	1.10	1.22	1.16
		2050	5338	5868	5595	1.20	1.32	1.25
		2070	5125	6160	5738	1.15	1.38	1.29
	8.5	2030	4748	5428	5137	1.06	1.22	1.15
		2050	5394	6262	5853	1.21	1.40	1.31
		2070	5337	7012	6273	1.20	1.57	1.41
CF	4.5	2030	2882	3591	3152	1.04	1.30	1.14
		2050	3113	3786	3518	1.13	1.37	1.27
		2070	2856	3963	3641	1.03	1.43	1.32
	8.5	2030	2482	3271	2961	0.90	1.18	1.07
		2050	3171	4196	3717	1.15	1.52	1.34
		2070	3707	5036	4533	1.34	1.82	1.64

precipitation occurred during the SW growing season, corresponding to 176 and 113 mm in CC and CCF, respectively.

3.3.2. Crop response to baseline environmental conditions

The zonal average SW season length was about 117 ± 9 days across both zones. The small variation of SW season length resulted from the simulated planting date based on the onset of favorable spring temperature.

The zonal average SW ET_a values were 308 ± 45 and 206 ± 47 mm in the CC and CCF zones, respectively. As with WW, ET_a for SW tended to be highest in the eastern part of the IPNW, and declined moving westward (Fig. 7-a, b). Given SW season precipitation values, 57% of ET_a came from SW season precipitation in the CC zone, and 55% in the CCF zone. There was a wide ET_a range across the area planted with SW (90 to 400 mm), ranging from 188 to 400 and 90 to 305 for the CC and CCF zones, respectively (Fig. 7-a, b). This large spatial fluctuation, although less than that for WW, will also have an important influence in the response to climate change and elevated atmospheric CO_2. The average SW baseline TUE was 4.2 ± 0.3 and 4.5 ± 0.37 g biomass kg water^{-1}, with the higher value obtained for CCF (Fig. 8-a, b), which are lower compared to TUE for WW due to higher temperature and vapor pressure deficit during the SW growing season providing less favorable conditions for TUE (Kremer et al., 2008). As with WW, SW TUE tended to be higher in the southern portion of each zone. In both CC and CCF zones, areas with lower precipitation have lower ET_a, higher crop water stress, and higher TUE for SW. The zonal average water stress index during the SW growing season were 0.19 and 0.35 in CC and CCF, which indicate higher water stress than during WW growing season.

SW yield was usually less than WW since the growing season was much shorter and water stress was higher. The baseline zonal average SW yield across the CC and CCF zones were 3503 ± 859 and 2169 ± 783 kg ha^{-1}, respectively.

3.4. Spring wheat: Future periods

3.4.1. Environmental conditions

Fig. 6-c, d shows the zonal average season temperature for the period 2015–2085 over the 12 GCMs for the CC and CFF zones. Zonal average growing season temperature will not change noticeably in

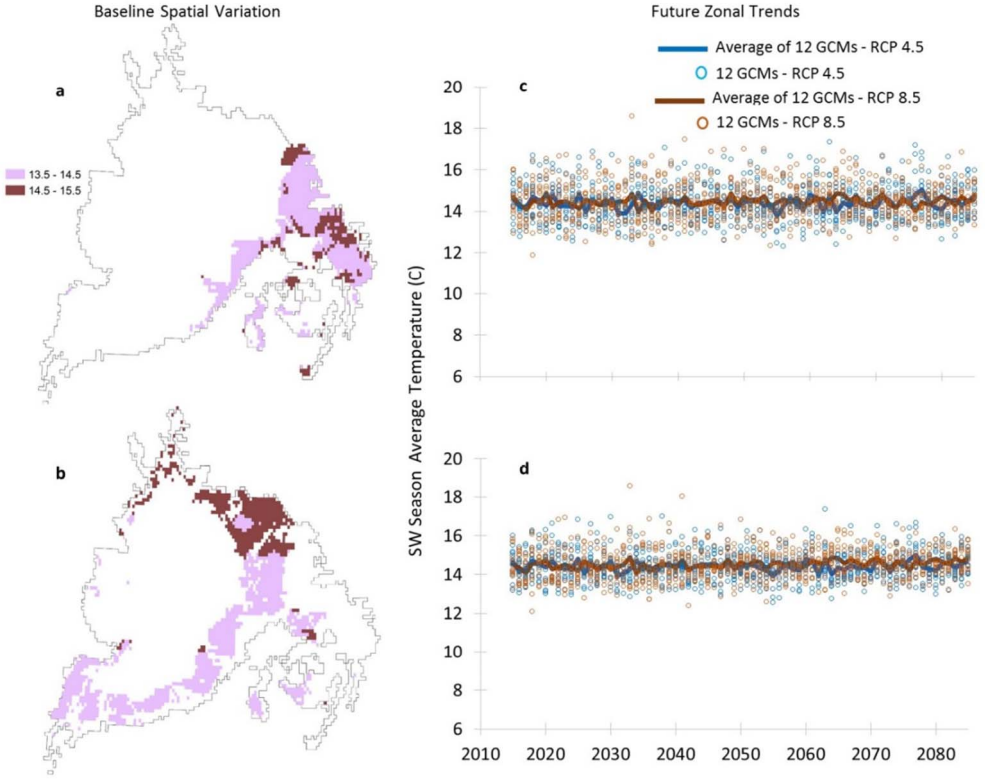

Fig. 6. Spatial distribution of baseline (1980–2010) average temperature during the spring wheat (SW) growing season for the continuous cropping (a) and annual crop-fallow transition (b) agroecological zones (AEZ), and future SW season temperature trends for the same AEZs (c, d), averaged over 12 general climate models (GCMs), for 2 atmospheric CO_2 representative concentration pathways (RCP) for the Inland Pacific Northwest. (1.5 column-colored).

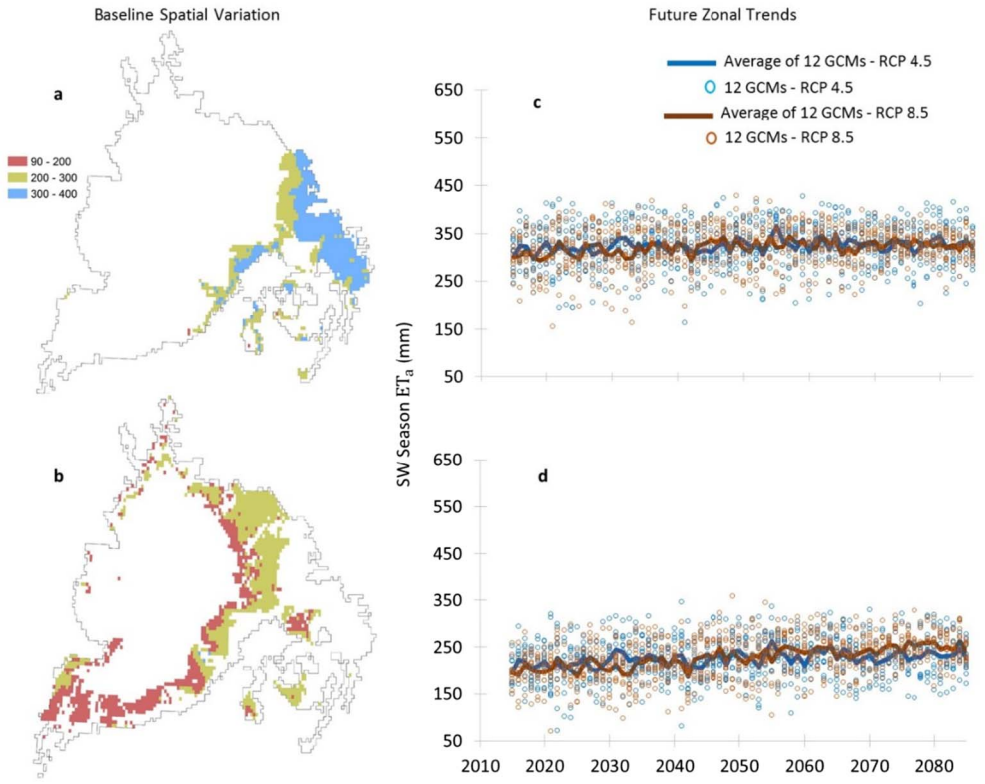

Fig. 7. Spatial distribution of baseline (1980–2010) evapotranspiration (ET_a) during the spring wheat (SW) growing season for the continuous cropping (a) and annual crop-fallow transition (b) agroecological zones (AEZ), and future SW season ET_a trends for the same AEZs (c, d) averaged over 12 general climate models (GCMs) and 2 atmospheric CO_2 representative concentration pathways (RCP) for the Inland Pacific Northwest. (1.5 column-colored).

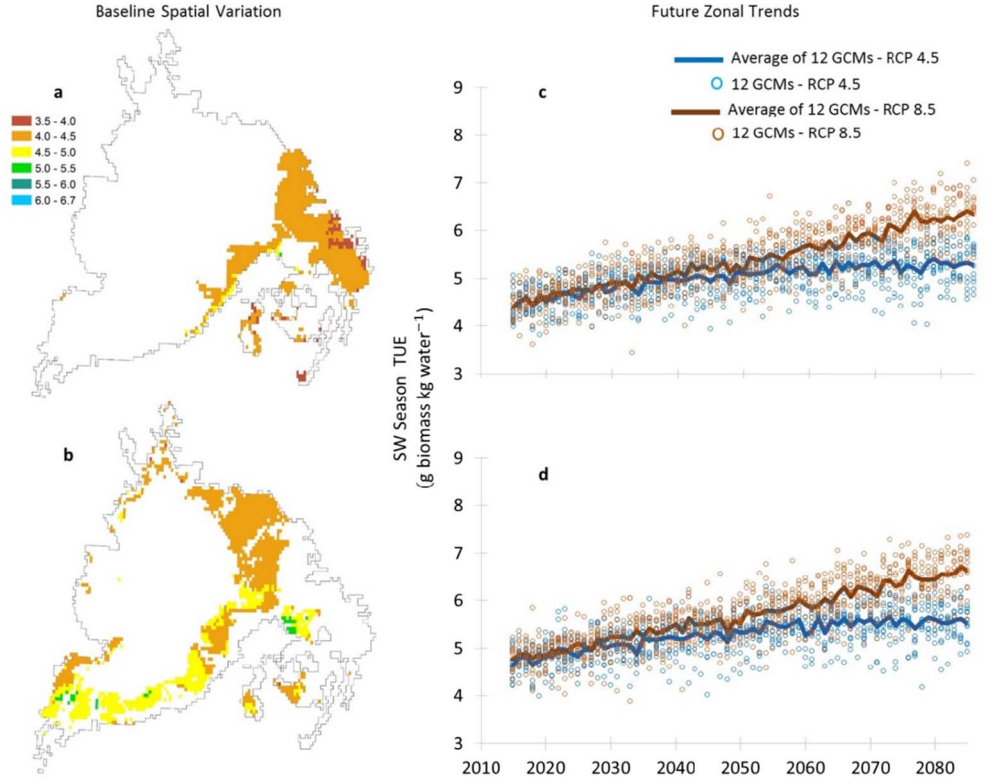

Fig. 8. Spatial distribution of baseline (1980–2010) transpiration use efficiency (TUE) during the spring wheat (SW) growing season for the continuous cropping (a) and annual crop-fallow transition (b) agroecological zones (AEZ), and future SW season TUE trends for the same AEZs (c, d), averaged over 12 general climate models (GCMs), for 2 atmospheric CO_2 representative concentration pathways (RCP) for the Inland Pacific Northwest. (1.5 column-colored).

either zone based on average of 12 GCMs. (about 0.2 and 0.3 °C by the end of the 2070 period under RCP 8.5 in CC and CCF). This results from the variable simulated planting date of SW, which adapts the growing season to warming. The zonal average maximum temperature during the SW growing season will decrease slightly in CC and CCF, but the minimum temperature will increase (about 1 °C in the 2070 period under both RCPs), creating somewhat better growth conditions during early spring.

As discussed, annual precipitation in the region will increase about 7% and 11% by the end of 2070s under RCP 4.5 and 8.5, respectively, at both CC and CCF zones. The average of 12 GCMs project that the proportion of zonal annual precipitation that will occur during the SW season will increase from 30% during the baseline period to 36 and 35% in CC and CCF respectively by the 2070s under RCP 4.5 and increase even more under the RCP 8.5 scenario (about 38 and 36%). These increases in SW season precipitation will lead to more favorable conditions for growth.

3.4.2. Wheat response to future environmental conditions

The zonal average SW season length will be similar to the baseline period in both zones due to the simulated earlier planting as temperature increases. The zonal average of SW ET_a will stay in the same range as baseline under both RCPs in CC and increase toward the end of the 2070s in CCF (Fig. 7). These increases in ET_a at the end of 2070s period compared to the beginning of the 2030s are about 7 and 26% at CC and CCF under RCP 8.5 (Fig. 7-c, d). These increases stem from a slight increase in seasonal precipitation and the midcentury winter wheat ET_a decline that will conserve water for use by SW.

TUE will increase toward the 2070s (Fig. 8). This is the result of the CO_2 fertilization effect, which increases photosynthesis (Ainsworth and Long, 2005) and reduces crop water use (Kimball et al., 1999). The zonal average TUE will reach 5.2 and 5.5 g biomass kg water^{-1} at 2070s under RCP 4.5 and 5.9 and 6.2 g biomass kg water^{-1} under RCP 8.5, in CC and CCF respectively. RCP 8.5 and CCF will be higher because the CO_2 fertilization effect will be more effective in drier regions. TUE will increase about 0.8 and 1.7 g biomass kg water^{-1} at the end of 2070s under RCP 4.5 and 8.5 respectively in both zones compared to the beginning of the 2030s (Fig. 8-c, d).

Table 4 presents the zonal SW, yields and R values averaged over all GCMs, and the maximum and minimum of all GCMs in each category. The zonal average SW yields will increase toward the 2070s. The favorable conditions provided by CO_2 fertilization, accompanied by more precipitation during the growing season, will cause the increase in yield compared to the baseline period. This positive effect is higher under RCP 8.5 than RCP 4.5, and is higher in the CCF zone than the CC zone. Ainsworth and Long (2005) reported a 17% yield increase with atmospheric CO_2 elevated to 550 ppm and no water limitation. Under RCP 4.5 (Table 4), our results at a comparable elevated CO_2 indicate roughly a 22 to 53% increase in SW yield, depending on AEZ. Greater yield increase due to CO_2 fertilization under water stress has been reported (Grant et al., 1999; Manderscheid and Weigel, 2007). The increases in R are higher under RCP 8.5 for 2050s and 2070s and are slightly less for 2030s compared to RCP 4.5. Lower increase of R in 2030s under RCP 8.5 occurs as a result of higher temperature, while the CO_2 concentration and its fertilization effect is similar in both RCPs. Later, toward the mid-century and 2070s, the CO_2 fertilization effect compensates for the negative effect of temperature and eventually higher atmospheric CO_2 concentration in this scenario will increase the R more compared to RCP 4.5.

3.5. Spatial distribution of yields

In addition to the projected mean yields and the range given by the minimum and maximum, which indicate the uncertainty due to GCMs, (Tables 3 and 4), it is interesting to evaluate how future yields may change across each zone. As discussed, precipitation and temperature conditions fluctuate significantly within each zone, both in the baseline data and in the 24 projected scenarios (12 GCMs × 2 RCPs). This heterogeneity will result in significant differences in crop responses so that the impact of climate change will differ not only between zones but also within zones.

Figs. 9 and 10 show histograms of the percent of grid cells in each AEZ that fall within given categories of yield for baseline, 2030s, 2050s and 2070s, indicating a large spatial variation of yields not only between zones, but also within zones.

For WW in the CC zone, the shift in modal yield and the distribution toward high yields by the 2070s may be an indication that further yield improvement is limited more by crop genetics than by the environment. Although the CC zone has more variability (among GCMs) in precipitation and, historically, a larger range of precipitation than the other AEZs (Fig. 3), the shorter growing season and milder winter temperatures may allow the crop to take near-full advantage of its genetic potential. Further yield improvement may be possible, but the improvement would require new cultivars analogous to the improvement of modern cultivars over landraces as reported by Sanchez-Garcia et al. (2013). With CropSyst, development of new cultivars could be simulated by adjusting crop parameters, but such an exercise was beyond the objectives of the current study.

The CCF zone historically has had a wider range of temperature than the CF zone, and this difference is likely to persist into the future. Also, the ensemble of GCMs suggest greater variability in precipitation within the zone than in CF. For these reasons, a more uniform

Table 4
Zonal spring wheat yield and future to baseline yield ratio averaged across 12 global climate models (GCM) and minimum and maximum of all GCMs for a given response variable for 2 representative concentration pathways (RCP) in the inland Pacific Northwest. Each period is 31 years, centered on the nominal value, and the zones are the continuous cropping (CC), annual crop-fallow transition (CCF) and crop-fallow (CF) agroecological zones.

Zone	RCP	Period	Yield (kg ha^{-1})			Ratio of future to baseline yield		
			Min	Max	Average	Min	Max	Average
CC	4.5	2030	3907	4763	4258	10.12	10.35	10.22
		2050	4013	5143	4638	10.15	10.47	10.32
		2070	4349	5224	4842	10.24	10.49	10.38
	8.5	2030	3895	4651	4172	10.11	10.33	10.19
		2050	4148	5287	4870	10.18	10.51	10.39
		2070	4435	5961	5396	10.27	10.70	10.54
CCF	4.5	2030	2474	2887	2715	10.14	10.33	10.25
		2050	2762	3508	3092	10.27	10.62	10.43
		2070	2960	3650	3309	10.36	10.68	10.53
	8.5	2030	2424	2745	2586	10.12	10.27	10.19
		2050	2661	3700	3368	10.23	10.71	10.55
		2070	3670	4549	4136	10.69	20.10	10.91

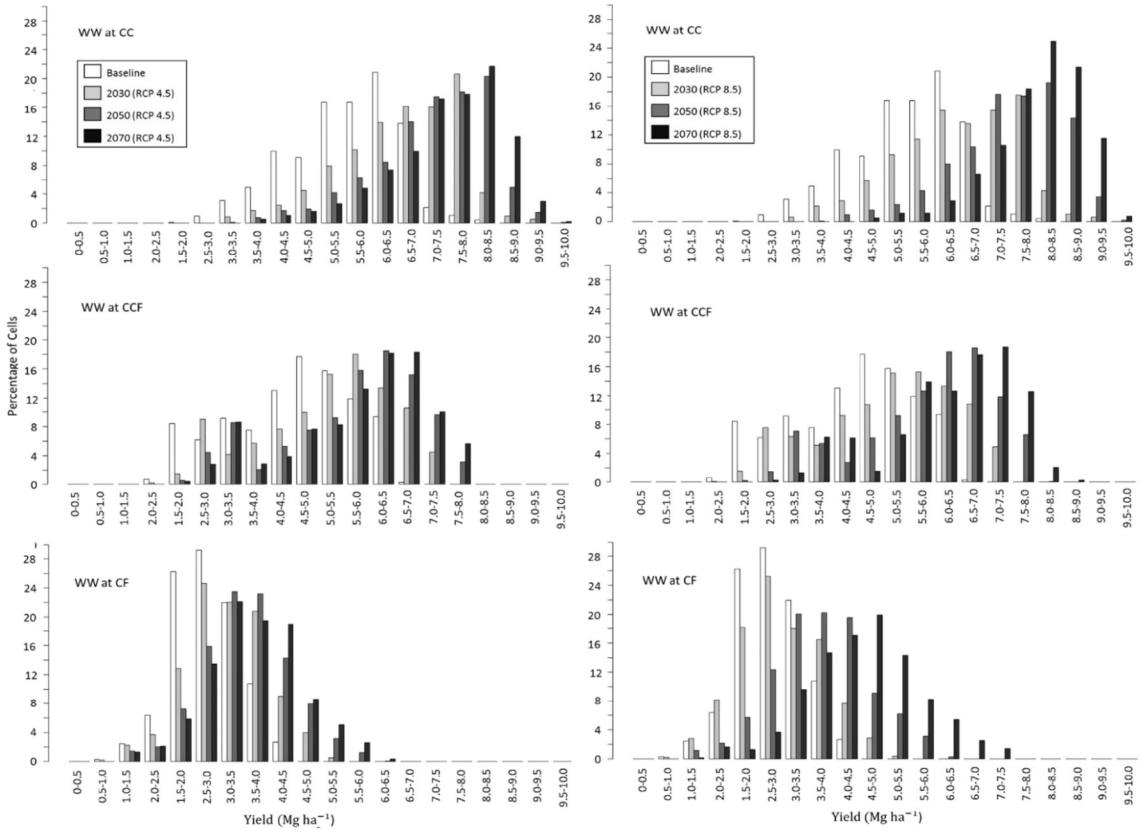

Fig. 9. Percentage of grid cells (y-axis) within the continuous cropping (CC), annual crop-fallow transition (CCF) and crop-fallow (CF) agroecological zones (AEZ) that yielded winter wheat (WW) in the specified range (x-axis). Data were averaged within the baseline period (1980–2010), or within 3 31-year future time periods centered on the nominal year in the legend. For the future projections, data were averaged over 12 general climate models within 2 atmospheric CO_2 representative concentration pathways (RCP) for the Inland Pacific Northwest.

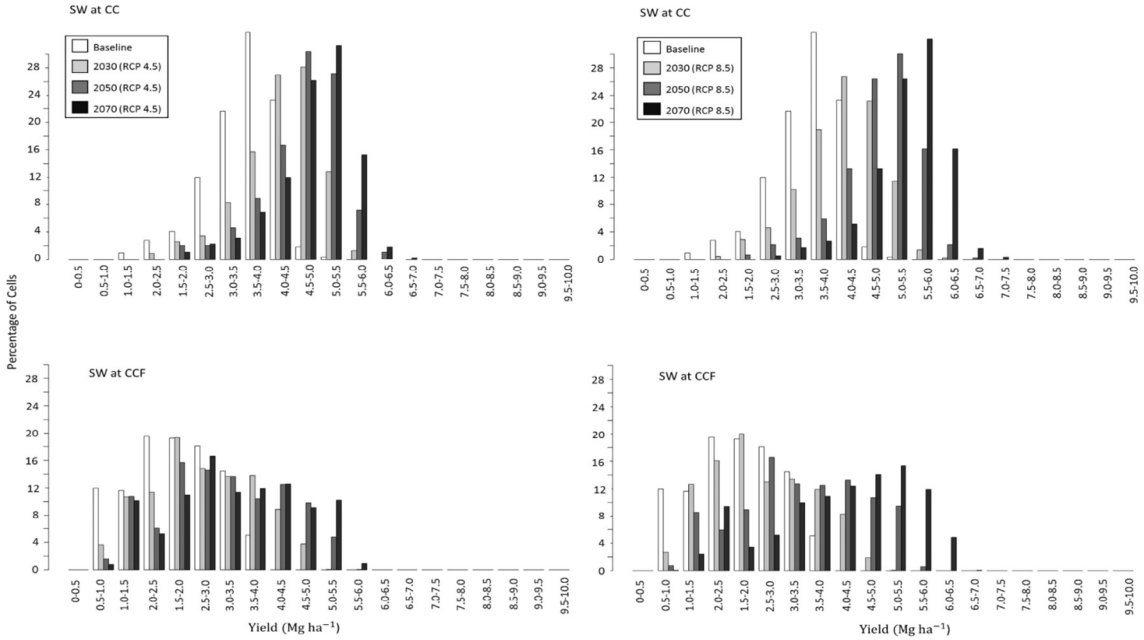

Fig. 10. Percentage of grid cells (y-axis) within the continuous cropping (CC), annual crop-fallow transition (CCF) and crop-fallow (CF) agroecological zones (AEZ) that yielded spring wheat (SW) in the specified range (x-axis). Data were averaged within the baseline period (1980–2010), or within 3 31-year future time periods centered on the nominal year in the legend. For the future projections, data were averaged over 12 general climate models within 2 atmospheric CO_2 representative concentration pathways (RCP) for the Inland Pacific Northwest.

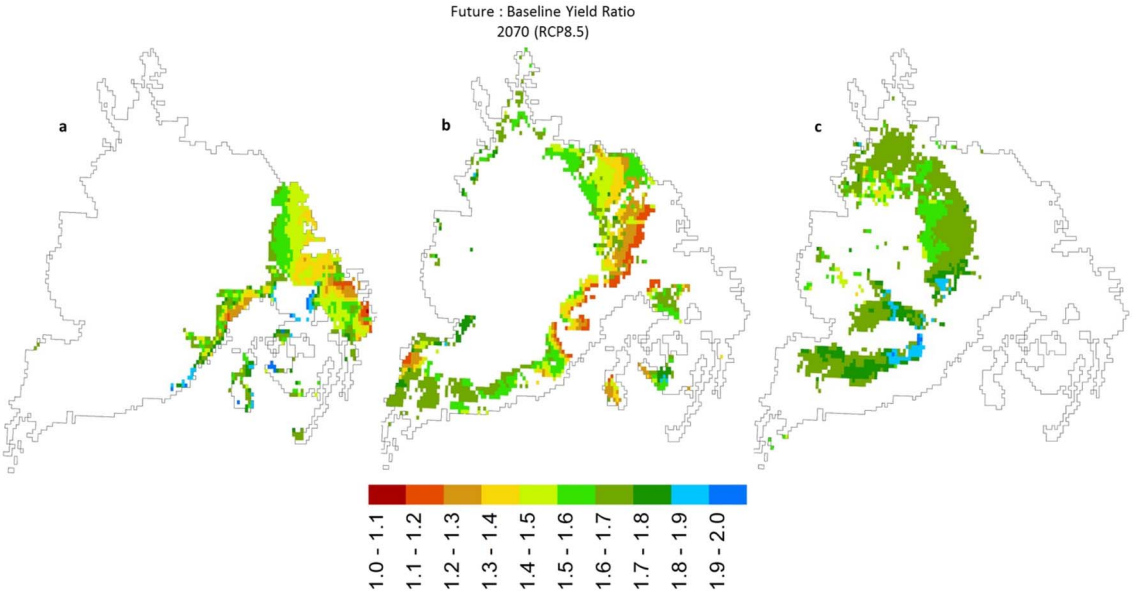

Fig. 11. Spatial distribution of 2070s to baseline winter wheat (WW) yield ratio for the continuous cropping (a) annual crop-fallow transition (b) and crop-fallow agroecological zones (AEZs) averaged over 12 general climate models (GCMs), for atmospheric CO_2 representative concentration pathways (RCP) 8.5 for the Inland Pacific Northwest.

distribution of WW yield into the future (Fig. 9) might be expected.

For WW in the CF zone, the normal distribution of future yield suggests that there are relatively few outlier environments, and that multiple stresses have restricted yield to the modal yield categories shown in Fig. 9.

Like WW, future SW yield in the CC zone shows a similar distribution toward high yields, which again suggests a genetic limitation to further yield improvement. The wide range of environments in the CCF zone would be expected to result in the most uniform distribution of yields (Fig. 10).

The large spatial variation of yield projections across the region and within zones is also true for the ratio of future to baseline yield, as illustrated in Fig. 11 for WW in the 3 zones during the 2070s time period under RCP 8.5. Although the overall trend is positive, variations in environmental conditions and soil characteristics will dictate that the larger average productivity projected for wheat in the future will not be shared equally by all growers in the region. Another implication is that some portions of a given zone may be better suited in the future, both from economic and environmental standpoints, to cropping systems traditionally adapted to a different zone.

4. Conclusions

Our results showed that climate change will have a positive effect on WW and SW yields over most parts of the IPNW. Although warming may tend to reduce wheat production globally (Asseng et al., 2015), increased atmospheric CO_2 could compensate for this negative effect in the dryland IPNW. In our study area the increase in temperature is projected to be more noticeable during the winter season and will therefore lead to more favorable WW growth conditions during the winter. WW season length will decrease toward 2085 and will be shorter under RCP 8.5. A shorter growing season may help prevent heat stress at the grain filling stage, while increased TUE will increase productivity. SW growing season temperatures are not projected to change much due to increasingly earlier planting so heat stress is not likely to affect SW yields more than baseline occurrences. The SW growing season maximum temperature will decrease and minimum temperature will increase, causing a better condition for SW compared to baseline. Much of the favorable SW response to climate change in our simulation was due to shifts in planting dates to account for shifts in climate. Adaptations to new climate norms, such as adjusted planting dates and better adjusted cultivars, will be a critical component of farm success and sustainability in the future. Annual precipitation will increase some which, along with the shorter growing season and lower ET_a in the CC and CCF zones, will leave more soil moisture at the end of the WW growing season. In CF there will be a small increase in ET_a for WW at the end of 2070s since increases in precipitation will be utilized for ET_a in this driest zone. Spring wheat ET_a will stay in the same range as baseline under both RCPs in CC, and will slightly increase toward the end of the 2070s in CCF as a result of increases in seasonal precipitation. TUE will increase as a result of a greater CO_2 fertilization effect for both WW and SW across the region, and slightly more for RCP 8.5 and for WW. Higher TUE leads to greater biomass and yield gains, an effect that is greater as water stress increases. These favorable conditions have the potential to increase the WW yield from 1.29 to 1.35 times by the end of the 2070s under RCP 4.5 and from 1.41 to 1.64 times under RCP 8.5, depending on zone. Since water stress is higher in SW than WW, yield increase values will tend to be higher for SW, ranging from 1.38 to 1.53 under RCP 4.5 and 1.54 to 1.91 under RCP 8.5. However, the WW and SW yield gains will not be distributed equally across the region and even within AEZs. The substantial climatic heterogeneity of the study area will influence where within a zone the most favorable outcomes will occur, suggesting that the larger average productivity projected for wheat in the future will not be shared equally by all growers.

Acknowledgements

This research was supported by the United States Department of Agriculture's National Institute of Food and Agriculture, Award #2011-68002-30191 for the project, Regional Approaches to Climate Change for Pacific Northwest Agriculture.

References

Abatzoglou, J.T., 2013. Development of gridded surface meteorological data for ecological applications and modelling. Int. J. Climatol. 33, 121–131. http://dx.doi.org/10.1002/joc.3413.

Abatzoglou, J.T., Brown, T.J., 2012. A comparison of statistical downscaling methods suited for wildfire applications. Int. J. Climatol. 32, 772–780. http://dx.doi.org/10.1002/joc.2312.

Ainsworth, E.A., Long, S.P., 2005. What have we learned from 15 years of free-air CO_2 enrichment (FACE) a meta-analytic review of the responses of photosynthesis, canopy properties and plant production to rising CO_2. New Phytol. 165, 351–372. http://dx.doi.org/10.1111/j.1469-8137.2005.01224.x.

Allen, L.H., 1990. Plant responses to rising carbon dioxide and potential interactions with air pollutants. J. Environ. Qual. 19, 15–34.
Asseng, S., Foster, I., Turner, N.C., 2011. The impact of temperature variability on wheat yields. Glob. Change Biol. 17, 997–1012. http://dx.doi.org/10.1111/j.1365-2486.2010.02262.x.
Asseng, S., Ewert, F., Martre, P., Rötter, R.P., Lobell, D.B., Cammarano, D., Kimball, B.A., Ottman, M.J., Wall, G.W., White, J.W., Reynolds, M.P., Alderman, P.D., Prasad, P.V.V., Aggarwal, P.K., Anothai, J., Basso, B., Biernath, C., Challinor, A.J., De Sanctis, G., Doltra, J., Fereres, E., Garcia-Vila, M., Gayler, S., Hoogenboom, G., Hunt, L.A., Izaurralde, R.C., Jabloun, M., Jones, C.D., Kersebaum, K.C., Koehler, A.-K., Müller, C., Naresh Kumar, S., Nendel, C., O'Leary, G., Olesen, J.E., Palosuo, T., Priesack, E., Eyshi Rezaei, E., Ruane, A.C., Semenov, M.A., Shcherbak, I., Stöckle, C., Stratonovitch, P., Streck, T., Supit, I., Tao, F., Thorburn, P.J., Waha, K., Wang, E., Wallach, D., Wolf, J., Zhao, Z., Zhu, Y., 2015. Rising temperatures reduce global wheat production. Nat. Clim. Chang. 5, 143–147. http://dx.doi.org/10.1038/nclimate2470.
Bocchiola, D., Nana, E., Soncini, A., 2013. Impact of climate change scenarios on crop yield and water footprint of maize in the Po valley of Italy. Agric. Water Manag. 116, 50–61. http://dx.doi.org/10.1016/j.agwat.2012.10.009.
Conley, M.M., Kimball, B.A., Brooks, T.J., Pinter, P.J., Hunsaker, D.J., Wall, G.W., Adam, N.R., LaMorte, R.L., Matthias, A.D., Thompson, T.L., Leavitt, S.W., Ottman, M.J., Cousins, A.B., Triggs, J.M., 2001. CO_2 enrichment increases water-use efficiency in sorghum. New Phytol. 151, 407–412.
Creighton, J., Strobel, M., Hardegree, S., Steele, R., Van Horne, B., Gravenmier, B., Horne, V., Owen, D., Peterson, L., Hoang, N.L., Bochicchio, J., Hall, W., Cole, M., Hestvik, S., Olson, J., 2015. In: Perry, A. (Ed.), Northwest Regional Climate Hub Assessment of Climate Change Vulnerability and Adaptation and Mitigation Strategies. United States Department of Agriculture (52 pp).
Dalton, M.M., Mote, P.W., Snover, A.K. (Eds.), 2013. Climate Change in the Northwest. Island Press/Center for Resource Economics, Washington, DC.
Donatelli, M., Srivastava, A.K., Duveiller, G., Niemeyer, S., Fumagalli, D., 2015. Climate change impact and potential adaptation strategies under alternate realizations of climate scenarios for three major crops in Europe. Environ. Res. Lett. 10, 75005. http://dx.doi.org/10.1088/1748-9326/10/7/075005.
Douglas, C.L.J., Rickman, R.W., Klepper, B.L., Zuzel, J.F., 1992. Agroclimatic zones for dryland winter wheat producing areas of Idaho, Washington, and Oregon. Northwest Sci. 66, 26–34.
Drake, B.G., Gonzàlez-Meler, Long, M.A., 1997. More efficient plants: a consequence of rising atmospheric CO_2? Annu. Rev. Plant Physiol. Plant Mol. Biol. 48, 609–639. http://dx.doi.org/10.1146/annurev.arplant.48.1.609.
Ericksen, P.J., Ingram, J.S.I., Liverman, D.M., 2009. Food security and global environmental change: emerging challenges. Environ. Sci. Pol. 12, 373–377. http://dx.doi.org/10.1016/j.envsci.2009.04.007.
Grant, R.F., Wall, G.W., Kimball, B.A., Frumau, K.F.A., Pinter Jr., P.J., Hunsaker, D.J., Lamorte, R.L., 1999. Crop water relations under different CO_2 and irrigation: Testing of ecosys with the free air CO_2 enrichment (FACE) experiment. Agric. For. Meteorol. 95, 27–51. http://dx.doi.org/10.1016/S0168-1923(99)00017-9.
Huggins, D.R., Rupp, R., Gessler, P., Pan, W., Brown, D.J., Machado, S., Walden, V.P., Eigenbrode, S., Abatzoglou, J.T., 2011. Dynamic Agroecological Zones for the Inland Pacific Northwest, USA. AGU Fall Meet. Abstr. 12. https://www.reacchpna.org/files/4613/5282/7467/AEZ_ASA_2012.pdf.
Jalota, S.K., Vashisht, B.B., 2016. Adapting cropping systems to future climate change scenario in three agro-climatic zones of Punjab, India. ResearchGate 18, 48–56.
Kimball, B.A., LaMorte, R.L., Pinter, P.J., Wall, G.W., Hunsaker, D.J., Adamsen, F.J., Leavitt, S.W., Thompson, T.L., Matthias, A.D., Brooks, T.J., 1999. Free-air CO_2 enrichment and soil nitrogen effects on energy balance and evapotranspiration of wheat. Water Resour. Res. 35, 1179–1190.
Kremer, C., Stöckle, C.O., Kemanian, A.R., Howell, T., 2008. Using a canopy transpiration and photosynthesis model for the evaluation of simple models of crop productivity. In: Ahuja, L.R., Reddy, V.R., Saseendran, S.A., Yu, Q. (Eds.), Advances in Agricultural Systems Modeling 1. ASA-SSSA-CSSA, Madison, WI.
Kristensen, K., Schelde, K., Olesen, J.E., 2011. Winter wheat yield response to climate variability in Denmark. J. Agric. Sci. 149, 33–47. http://dx.doi.org/10.1017/S0021859610000675.
Laurila, H., 2008. Simulation of spring wheat responses to elevated CO_2 and temperature by using CERES-wheat crop model. Agric. Food Sci. 10, 175–196.
Lipiec, J., Doussan, C., Nosalewicz, A., Kondracka, K., 2013. Effect of drought and heat stresses on plant growth and yield: a review. Int. Agrophysics 27, 463–477. http://dx.doi.org/10.2478/intag-2013-0017.
Long, S.P., Ainsworth, E.A., Rogers, A., Ort, D.R., 2004. Rising atmospheric carbon dioxide: plants FACE the future. Annu. Rev. Plant Biol. 55, 591–628.
Manderscheid, R., Weigel, H.-J., 2007. Drought stress effects on wheat are mitigated by atmospheric CO_2 enrichment. Agron. Sustain. Dev. 27, 79–87. http://dx.doi.org/10.1051/agro:2006035.
O'Leary, G.J., Walker, S., Joshi, N., White, J.W., 2011. Chapter 4: Water Availability and Use in Rainfed Farming Systems, Their relationship to System Structure, Operation and Management. In Book Rainfed Farming Systems, pp. 101–132 [WWW Document]. URL. https://www.researchgate.net/publication/226053504_Water_Availability_and_Use_in_Rainfed_Farming_Systems (accessed 8.24.16).
O'Leary, G.J., Christy, B., Nuttall, J., Huth, N., Cammarano, D., Stöckle, C., Basso, B., Shcherbak, I., Fitzgerald, G., Luo, Q., Farre-Codina, I., Palta, J., Asseng, S., 2014. Response of wheat growth, grain yield and water use to elevated CO_2 under a free-air CO_2 enrichment (FACE) experiment and modelling in a semi-arid environment. Glob. Change Biol. http://dx.doi.org/10.1111/gcb.12830.
Olesen, J.E., Trnka, M., Kersebaum, K.C., Skjelvåg, A.O., Seguin, B., Peltonen-Sainio, P., Rossi, F., Kozyra, J., Micale, F., 2011. Impacts and adaptation of European crop production systems to climate change. Eur. J. Agron. 34, 96–112. http://dx.doi.org/10.1016/j.eja.2010.11.003.
Ortiz, R., Sayre, K.D., Govaerts, B., Gupta, R., Subbarao, G.V., Ban, T., Hodson, D., Dixon, J.M., Iván Ortiz-Monasterio, J., Reynolds, M., 2008. Climate change: Can wheat beat the heat? Agric. Ecosyst. Environ. 126, 46–58. International Agricultural Research and Climate Change: A Focus on Tropical Systems http://dx.doi.org/10.1016/j.agee.2008.01.019.
Papendick, R.I., 1996. Farming systems and conservation needs in the Northwest Wheat Region. Am. J.
Sanchez-Garcia, M., Royo, C., Aparicio, N., Martín-Sánchez, J.A., Alvaro, F., 2013. Genetic improvement of bread wheat yield and associated traits in Spain during the 20th century. J. Agric. Sci. 151, 105–118. http://dx.doi.org/10.1017/S0021859612000330.
Schillinger, W.F., Papendick, R.I., 2008. Then and now: 125 years of dryland wheat farming in the Inland Pacific Northwest. Agron. J. 100 (Suppl), S166–S182.
Schillinger, W.F., Papendick, R.I., Guy, S.O., Rasmussen, P.E., Kessel, C.V., 2003. Dryland Cropping in the Western United States. Pac. Northwest Conserv. Tillage Handb. Ser. No 28. (Chapter 2).
Schillinger, W.F., Papendick, R.I., Guy, S.O., Rasmussen, P.E., van Kessel, C., 2006. Dryland cropping in the western United States. In: Peterson, G.A., Unger, P.W., Payne, W.A. (Eds.), Dryland Agriculture, second ed. ASA, CSSA, and SSSA, Madison, WI, pp. 365–393 Agronomy monograph no 23.
Semenov, M.A., Shewry, P.R., 2011. Modelling predicts that heat stress, not drought, will increase vulnerability of wheat in Europe. Sci. Rep. 1, 66.
Shewry, P.R., Hey, S.J., 2015. The contribution of wheat to human diet and health. Food Energy Secur. 4, 178–202. http://dx.doi.org/10.1002/fes3.64.
Sommer, R., Glazirina, M., Yuldashev, T., Otarov, A., Ibraeva, M., Martynova, L., Bekenov, M., Kholov, B., Ibragimov, N., Kobilov, R., Karaev, S., Sultonov, M., Khasanova, F., Esanbekov, M., Mavlyanov, D., Isaev, S., Abdurahimov, S., Ikramov, R., Shezdyukova, L., de Pauw, E., 2013. Impact of climate change on wheat productivity in Central Asia. Agric. Ecosyst. Environ. 178, 78–99. http://dx.doi.org/10.1016/j.agee.2013.06.011.
Stöckle, C.O., Jara, J., 1998. Modeling transpiration and soil water content from a corn (Zea Maize L.) field: 20 min vs. daytime integration step. Agric. For. Meteorol. 92, 119–130.
Stöckle, C.O., Martin, S.A., Campbell, G.S., 1994. CropSyst, a cropping systems simulation model: Water/nitrogen budgets and crop yield. Agric. Syst. 46, 335–359. http://dx.doi.org/10.1016/0308-521X(94)90006-2.
Stöckle, C.O., Donatelli, M., Nelson, R., 2003. CropSyst, a cropping systems simulation model. Eur. J. Agron. 18, 289–307. Modelling Cropping Systems: Science, Software and Applications http://dx.doi.org/10.1016/S1161-0301(02)00109-0.
Stöckle, C.O., Nelson, R.L., Higgins, S., Brunner, J., Grove, G., Boydston, R., Whiting, M., Kruger, C., 2010. Assessment of climate change impact on Eastern Washington agriculture. Clim. Chang. 102, 77–102. http://dx.doi.org/10.1007/s10584-010-9851-4.
Teixeira, E.I., Fischer, G., van Velthuizen, H., Walter, C., Ewert, F., 2013. Global hot-spots of heat stress on agricultural crops due to climate change. Agric. For. Meteorol. Agricultural prediction using climate model ensembles 170, 206–215. http://dx.doi.org/10.1016/j.agrformet.2011.09.002.
Thomson, A.M., Brown, R.A., Ghan, S.J., Izaurralde, R.C., Rosenberg, N.J., Leung, L.R., 2002. Elevation dependence of winter wheat production in Eastern Washington State with climate change: a methodological study. Clim. Chang. 54, 141–164. http://dx.doi.org/10.1023/A:1015743411557.
Thornley, J.H.M., 1998. Dynamic model of leaf photosynthesis with acclimation to light and nitrogen. Ann. Bot. 81, 421–430.
Torriani, D.S., Calanca, P., Schmid, S., Beniston, M., Fuhrer, J., 2007. Potential effects of changes in mean climate and climate variability on the yield of winter and spring crops in Switzerland. Clim. Res. 34, 59–69. http://dx.doi.org/10.3354/cr034059.
United Nations, 2015. World Population Prospects - Population Division. https://esa.un.org/unpd/wpp/publications/files/key_findings_wpp_2015.pdf.
USDA - National Agricultural Statistics Service [WWW document], n.d. URL https://www.nass.usda.gov/Research_and_Science/Cropland/Release/
Wilcox, J., Makowski, D., 2014. A meta-analysis of the predicted effects of climate change on wheat yields using simulation studies. Field Crops Res. 156, 180–190. http://dx.doi.org/10.1016/j.fcr.2013.11.008.
Yang, Y., Liu, D.L., Anwar, M.R., O'Leary, G., Macadam, I., Yang, Y., 2015. Water use efficiency and crop water balance of rainfed wheat in a semi-arid environment: sensitivity of future changes to projected climate changes and soil type. Theor. Appl. Climatol. 123, 565–579. http://dx.doi.org/10.1007/s00704-015-1376-3.
Zheng, B., Chenu, K., Fernanda Dreccer, M., Chapman, S.C., 2012. Breeding for the future: what are the potential impacts of future frost and heat events on sowing and flowering time requirements for Australian bread wheat (Triticum aestivum) varieties? Glob. Change Biol. 18, 2899–2914. http://dx.doi.org/10.1111/j.1365-2486.2012.02724.x.